

Electronic Structure and Photophysical Characteristics of Substituted 3-(2-Benzthiazolyl)-Coumarins and Coumarinimines

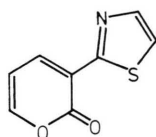
P. Nikolov ^a, N. Tyutyulkov ^a, and V. Dryanska ^b

Z. Naturforsch. **42a**, 987–993 (1987); received March 31, 1987

Dedicated to Professor Oskar E. Polansky on the occasion of his 67th birthday

The spectral properties of a group of 3-(2-benzthiazolyl)-coumarins and coumarinimines, some of them having high fluorescence quantum yield ($Q_f > 0.7$), are described.

The quantum-chemical investigations show that the main chromophore of this group of dyes is the 3-(2-thiazolyl)-2 H-pyran-2-one fragment



i.e. the coumarin (coumarinimine) and the benzthiazolyl fragments are not separate chromophores.

I. Introduction

The 3-benzthiazolyl-coumarins are widely used as laser dyes [1, 2, 3], fluorescent dyes [4], light collectors [2], etc. [5, 6].

The purpose of this paper is to study some new representatives of this group, as well as to elucidate theoretically the relationship between their electronic and photophysical properties.

Table 1 shows the compounds investigated. Their synthesis and chemical characteristics are described in [7].

II. Spectral Properties

The compounds investigated have been synthesized according to [7] and repeatedly recrystallized,

their purity being controlled by thin layer chromatography. The solvents used are of spectral grade. The absorption spectra are recorded on a double beam spectrophotometer Specord M40 (Carl Zeiss, Jena, GDR), the luminescence spectra are taken on a spectrofluorimeter Perkin-Elmer MPF-44B. The fluorescence lifetimes are measured on a nanosecond spectrofluorimeter PRA-2000. 3-amino-phthalimid ($Q_f = 0.6$ in ethanol [8]) is used as a fluorescence standard. The emission of the compounds in solid phase is measured at an angle $30^\circ/60^\circ$ between the normal to the surface and the exciting/emitted light. The low-temperature luminescence measurements are performed at 77 K in the standard phosphorescence accessory to MPF-44B.

IIa. UV-VIS absorption spectra

Table 2 shows some basic spectral characteristics of the studied compounds (the numbers of the substances correspond to those in Table 1). The longest-wavelength absorption band of all compounds in solution is in the region $22\,000\text{--}28\,000\text{ cm}^{-1}$, it is intensive (ϵ is about $20\,000\text{ l mol}^{-1}\text{ cm}^{-1}$ in $\text{C}_2\text{H}_5\text{OH}$) and has a well defined vibrational structure. At

^a Bulgarian Academy of Sciences, Institute of Organic Chemistry with Centre of Phytochemistry, 1113 Sofia, Bulgaria.

^b Faculty of Chemistry, University of Sofia, Department of Organic Chemistry, 1126 Sofia, Bulgaria.

Reprint requests to Dr. P. Nikolov, Bulgarian Academy of Sciences, Institute of Organic Chemistry with Centre of Phytochemistry, 1113 Sofia, Bulgaria.

0932-0784 / 87 / 0900-0987 \$ 01.30/0. – Please order a reprint rather than making your own copy.



Dieses Werk wurde im Jahr 2013 vom Verlag Zeitschrift für Naturforschung in Zusammenarbeit mit der Max-Planck-Gesellschaft zur Förderung der Wissenschaften e.V. digitalisiert und unter folgender Lizenz veröffentlicht: Creative Commons Namensnennung-Keine Bearbeitung 3.0 Deutschland Lizenz.

Zum 01.01.2015 ist eine Anpassung der Lizenzbedingungen (Entfall der Creative Commons Lizenzbedingung „Keine Bearbeitung“) beabsichtigt, um eine Nachnutzung auch im Rahmen zukünftiger wissenschaftlicher Nutzungsformen zu ermöglichen.

This work has been digitalized and published in 2013 by Verlag Zeitschrift für Naturforschung in cooperation with the Max Planck Society for the Advancement of Science under a Creative Commons Attribution-NoDerivs 3.0 Germany License.

On 01.01.2015 it is planned to change the License Conditions (the removal of the Creative Commons License condition “no derivative works”). This is to allow reuse in the area of future scientific usage.

N°	X	Y	Z
1	NH	H	H
3	NH	H	Br
4	NH	OH	H
5	NH	H	NO ₂
6	O	H	H
8	O	H	Br
9	O	OH	H
10	O	H	NO ₂

Table 1. Compounds investigated.

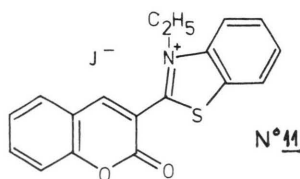
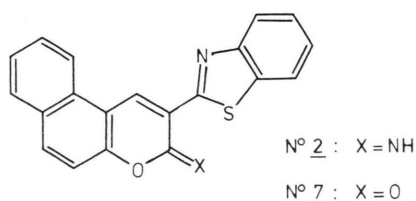
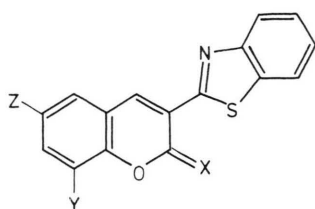
Table 2. Experimental spectral characteristics of the compounds investigated in solvents of different polarity at 293 K. ν^A , ν^F : energy of the Franck-Condon absorption and fluorescence transition, ϵ : molar absorptivity, (/: very poor solubility), Q_f : fluorescence quantum yield.

Table 2 a.

N°	Ethanol			
	ν^A [cm ⁻¹]	ϵ [l mol ⁻¹ cm ⁻¹]	ν^F [cm ⁻¹]	Q_f
1	27 120	19 050	21 980	0.042
2	23 720	21 260	19 920	0.21
3	27 000	18 390	21 460	0.04
4	27 960	22 200	21 010	0.002
5	27 520	16 880	21 740	< 10 ⁻³
6	27 560	32 950	21 810	0.17
7	24 360	25 280	20 830	0.73
8	27 240	16 600	21 550	0.09
9	27 600	27 340	22 030	< 10 ⁻³
10	27 300	/	20 620	0.01
11	27 360	/	21 950	0.008

shorter wavelengths there is a series of absorption transitions of lower intensity.

The comparison of the 3-(2-benzthiazolyl)-coumarins **6–10** with the corresponding 3-(2-benzthiazolyl)-coumarinimines shows that the replacement of the O atom with an NH group (heteroatom X, Fig. 1) practically does not influence the electronic spectra (the position of the bands, their vibrational structure and relative intensity, Table 2). In both groups of investigated compounds the OH group in position 8 (**4, 9**) leads to a blue shift of the Franck-Condon absorption transition, while a Br atom or an NO₂ group in position **6** (**3, 5, 8, 10**), as well as the condensed aromatic nucleus (**2, 7**), lowers the energy of the absorption transition. Most pronounced is this effect for compounds **2** and **7** (Table 2).

The computed transition energies and oscillator strengths, in the PPP-SCF-CI approximation, are denoted by vertical lines in Fig. 1 (see Section III).

Figure 1 shows also the results from the polarization studies of the fluorescence excitation spectra of **7** in frozen ethanolic solutions at 77 K, corrected for the instrumental response [9]. These results show that the polarization degree P_0 remains constant over the longest-wavelength absorption band and diminishes at shorter wavelengths.

The polarization data are in good agreement with the quantum-chemical calculations for the transition energies (Fig. 1) and show that the longest wavelength absorption band results from one $^1S_0 - ^1S_1$ ($\pi\pi^*$) transition. This conclusion is supported by the mirror symmetry relationship between the longest wavelength absorption band and the fluorescence spectrum.

Table 3 shows the angles β between the absorption and emission transition moments of compounds **1, 2, 6** and **7**, computed from the polarization excitation spectra according to [10].

The angle between the $^1S_0 - ^1S_1$ ($\pi\pi^*$) transition moment and the next $^1S_0 - ^1S_2$ ($\pi\pi^*$) and $^1S_0 - ^1S_3$ ($\pi\pi^*$) transition moments is very small for both the unsubstituted 3-(2-benzthiazolyl)-coumarin **6** (4°), and its imine **1** (6°). This angle is about 15° for the corresponding 5,6-benzoderivatives **7** and **2**; this value is close to the by the same method computed angle between the first two absorption transition moments of coumarin [11].

The $n\pi^*$ transitions of the studied benzthiazolyl derivatives of coumarin **6–10** and coumarinimine

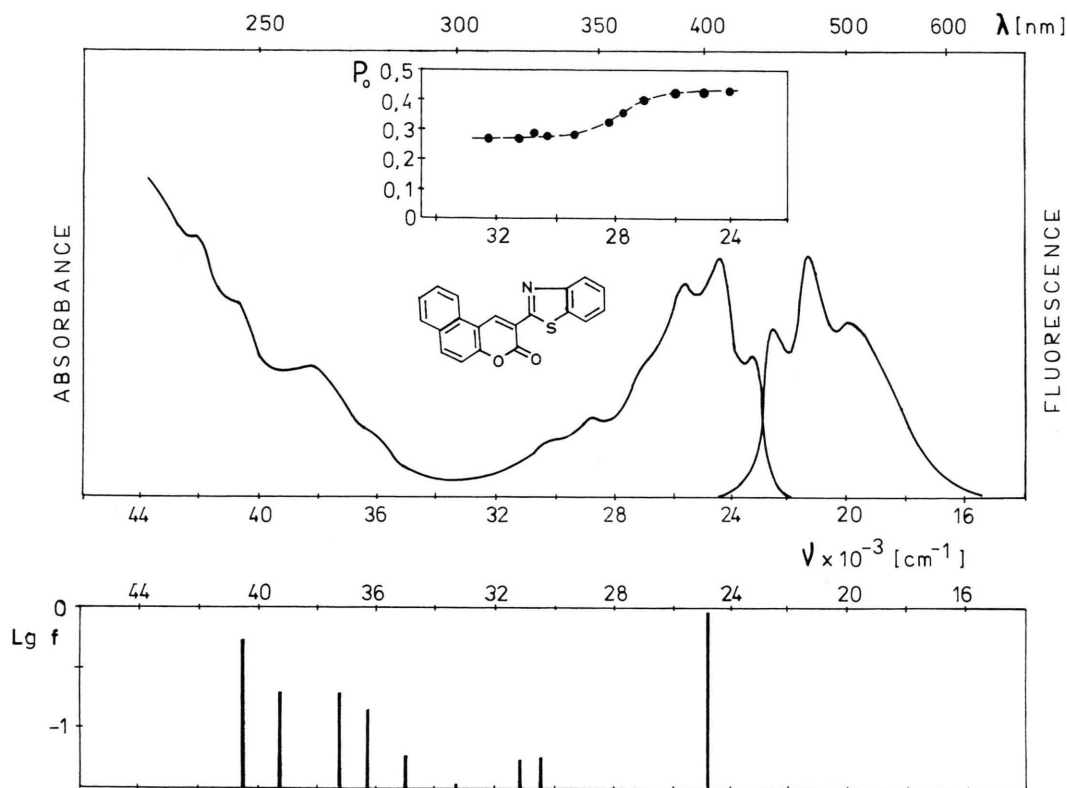


Fig. 1. Electronic spectra of **7** in ethanol at 293 K. (...): polarization degree P_0 in frozen ethanol solution at 77 K, computed from the polarized fluorescence excitation spectra according to [9]. The vertical lines denote the computed energy of the singlet $\pi\pi^*$ transitions and the corresponding oscillator strengths.

Table 2 b.

N°	Cyclohexane			1,4-Dioxan			Acetonitrile		
	ν^A	ν^F	Q_f	ν^A	ν^F	Q_f	ν^A	ν^F	Q_f
1	27 320	22 730	0.02	27 080	22 270	0.01	27 160	21 650	0.01
2	23 880	20 530	0.07	23 720	20 880	0.17	23 840	19 880	0.14
6	27 520	22 700	0.25	27 560	22 370	0.23	27 720	22 030	0.17
7	24 440	21 250	0.66	24 480	21 010	0.78	24 560	20 920	0.77

Table 3. The angles β_1 and β_2 between the directions of fluorescence (at ν^F) and the absorption transition moments (at ν_1^A and ν_2^A) determined from the polarized fluorescence excitation spectra of compounds **1**, **2**, **6**, **7** in ethanol at 77 K.

N°	ν^F	ν_1^A	β_1	ν_2^A	β_2
1	22 730	27 030	34°	34 480	40°
2	20 750	24 390	13°	29 410	29°
6	22 730	27 400	27°	33 330	30°
7	21 280	25 000	19°	30 300	34°

1–5, like those of the unsubstituted coumarin and many of its derivatives [11, 12], cannot be observed in the absorption spectra. However, the high fluorescence quantum yields of **7** and **2** show that the energy of the O–O transition of the lowest singlet $n\pi^*$ state is considerably higher than that of the $^1S_1(\pi\pi^*)$ state. As the length of the conjugated system slightly affects the energy of the localized $n\pi^*$ transitions [13], the energy of $^1S_1(n\pi^*)$ in the

investigated compounds can be evaluated by analogy with the unsubstituted coumarin: $E_{n\pi^*} > 32\,000\text{ cm}^{-1}$.

IIb. Luminescence characteristics

All of the studied compounds fluorescence in solution at room temperature [14]: Analogously to other substituted 3-(2-benzthiazolyl)-coumarins [1, 2, 3, 5], their fluorescence Franck-Condon transition ν^F is in the region $20\,000\text{--}22\,000\text{ cm}^{-1}$. The fluorescence band has a well-defined vibrational structure, mirror symmetrical to the longest wavelength absorption maximum; the corrected excitation spectrum is identical with the absorption one in the region $24\,000\text{--}46\,000\text{ cm}^{-1}$.

The fluorescence quantum yield Q_f strongly depends on the substituents *Y* and *Z*; it is highest for the 5,6-benzoderivatives **7** and **2**.

It is well-known [1, 4, 12] that the condensation of an aromatic nucleus in position 5,6 of the unsubstituted coumarin leads to a large red shift of the longest-wavelength absorption maximum and a considerable increase of the fluorescence quantum yield. However, the bathochromic shift of the longest-wavelength absorption $\pi\pi^*$ transition of the studied 3-(2-benzthiazolyl)-derivatives of coumarin (**6**–**10**) and coumarinimine (**1**–**5**) is not always accompanied by an increase of the fluorescence intensity. For example, upon quaternization of **6**, the Franck-Condon absorption transition moves about 200 cm^{-1} to the red, while the fluorescence quantum yield diminishes more than 10 times (Table 2).

The substitution of the NH group with an O atom leads to a similar effect: the slight bathochromic shift of the longest-wavelength absorption maximum of the m coumarinimines **1**–**5**, relative to that of the corresponding coumarins **5**–**10**, is accompanied by a decrease of Q_f . The largest difference – about 600 cm^{-1} , is observed for **2** and **7**; Q_f is 0.21 and 0.73, respectively (Table 2).

Our results are similar to those described in [12]: the replacement of the substituent in position 3 of the 5,6-benzo-coumarin, in the order COOH, COOC₂H₅, COOCH₃, leads to a decrease of the energy of the $^1S_0\text{--}^1S_1$ ($\pi\pi^*$) state: $\nu^A = 27\,400\text{ cm}^{-1}$, $26\,670\text{ cm}^{-1}$ and $25\,970\text{ cm}^{-1}$ in C₂H₅OH, which does not correlate with the change of Q_f ($Q_f = 0.37$, 0.42, 0.34, resp.).

Table 4 shows some luminescence characteristics of the studied compounds in frozen ethanolic solutions at 77 K. The fluorescence intensities of all the substances, except for **2** and **7** are from ten to fifty times greater in a frozen matrix than at room temperature, the fluorescence intensity of **2** increases about 3 times upon freezing while that of **7** remains practically constant. Usually, the enhancement of Q_f in a frozen solution is attributed to the absence of intramolecular vibrations (librations) of separate, weakly connected molecular fragments – in our case the benzthiazolyl and the coumarin fragments. However, the quantum-chemical calculations show that, for all the studied molecules, the order of the (C–C) bond connecting the two fragments substantially increases in the fluorescent 1S_1 ($\pi\pi^*$) state. This should hinder their libration and should thus decrease the probability for dissipation of the electronic energy along this vibrational degree of freedom.

Increasing the solvent polarity (C₆H₁₂, 1,4-dioxan, C₂H₅OH, CH₃CN) leads to only a small change in the Stokes shift (less than 1000 cm^{-1} , Table 2) and, according to Lippert's model [15], this means that the dipole moment change in the 1S_1 ($\pi\pi^*$) state is not more than 2D.

The fluorescence quantum yield of the compounds **1**–**10** only slightly depends on the solvent: there is no relationship between Q_f and the solvent polarity (Table 2).

Table 4. Spectral characteristics in frozen ethanol solution at 77 K and in solid phase. ν^F , ν^{ex} : energy of the fluorescence and the corresponding excitation maxima; the excitation spectra at 77 K and 273 K are identical. I^F : relative fluorescence intensity at ν^F .

N ^o	C ₂ H ₅ OH, 77 K		Solid phase, 293 K		
	ν^F	$\frac{I^F(77\text{ K})}{I^F(293\text{ K})}$	ν^{ex}	ν^F	$\frac{I^F}{I^F(\mathbf{6})}$
1	22 470	50	22 990	19 160	0.15
2	19 920	3	20 410	16 120	0.06
3	21 690	30	22 730	18 870	0.08
4	21 010	25	no emission		
5	21 700	25	22 730	18 080	0.13
6	22 270	10	23 530	20 410	1.00
7	21 280	1	21 740	18 450	0.34
8	22 120	30	25 510	20 410	0.23
9	22 030	30	22 470	18 870	0.06
10	21 500	10	24 100	19 420	0.08
11	21 030	10	23 150	15 630	0.02

Table 5. Decay time τ and constants of radiative (K_f) and nonradiative (K_{nf}) transitions, calculated from τ and Q_f in C_2H_5OH at 293 K. τ is calculated from the fluorescence decay curve, fitted to a monoexponential linear function $I(t) = A \exp(-t/\tau)$; χ : mean error of fitting; monochromatic excitation with ν^{ex} , monochromatic emission at ν^F . Dimensions: τ [ns], K [ns^{-1}], ν [cm^{-1}].

N°	τ	τ_f	K_f	K_{nf}	χ	A	ν^{ex}	ν^F
1	1.2	28.57	0.035	0.798	1.56	0.06	25 000	22 000
2	3.1	14.76	0.068	0.256	1.10	0.91	30 770	21 280
6	0.93	5.47	0.183	0.89	1.33	0.035	26 300	21 740
7	3.7	5.07	0.197	0.073	1.10	1.92	30 770	21 280

Table 5 shows the lifetime τ of the 1S_1 ($\pi\pi^*$) state, computed from the fluorescence decay curve, and the radiative and non-radiative transition constants, calculated from τ and Q_f .

Two of the compounds investigated (**4** and **10**) phosphorescence in frozen ethanolic solution at 77 K, the phosphorescence maxima are at 510 and 540 nm, respectively; the S–T splitting is about 3000 cm^{-1} ; the excitation phosphorescence and excitation fluorescence spectra are identical.

Although many coumarin derivatives are used as luminescent dyes and colourants for plastics and synthetic fibres (see e.g. [1, 2, 4]), there are few literature data for their fluorescent characteristics in solid phase [4, 16].

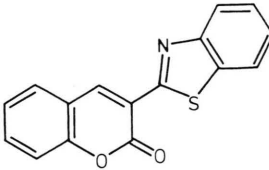
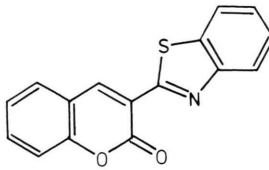
Table 4 gives the excitation and fluorescence maxima and the normalized to unity relative fluorescence intensities in solid phase. Most intensive is the solid phase emission of **6**; for comparison, the intensity of the fluorescence maximum of **7** in EtOH at 293 K at excitation wavelength $23\,200\text{ cm}^{-1}$, where the optical density is 0.1, is 35 times higher.

III. Quantum-chemical Investigations

All qualitative results are obtained by the Pariser-Parr-Pople (SCF-CI) method with a standard parametrization [17, 18], taking into account all singly-excited configurations. The C–C bond lengths are calculated using Hückel bond orders and the Coulson-Golebiewski formula [19].

The absorption spectra ($\pi\pi^*$ transitions) of all compounds investigated agree well with the quantum-chemical calculations. The difference between the calculated and the experimental Franck-Condon

Table 6. Computed energies ΔE [eV] and oscillator strengths f of the longest-wavelength $^1S_0 - S_1$ ($\pi\pi^*$) transitions of **6a** and **6b**.

			
6a		6b	
ΔE	f	ΔE	f
3.25	1.079	3.17	1.002
3.82	0.062	3.82	0.111
3.96	0.059	3.91	0.119
4.33	0.002	4.25	0.006
4.57	0.072	4.60	0.017
4.90	0.176	4.89	0.139
4.99	0.210	5.00	0.334

$\Delta E(^3T_1) = 1.21\text{ [eV]}, \Delta E(^3T_1) = 1.11\text{ [eV]}$
 $\Delta E_{exp} = 3.41\text{ [eV] (in } C_6H_{12})$

transition energies ν^A is within the accuracy of the PPP method. Figure 1 allows for comparison of the absorption spectrum of **7** and the calculated transition energies and oscillator strengths.

The compounds investigated may exist in two tautomeric forms; those for **6** are shown in Table 6. As the computed excitation energies and oscillator strengths of the tautomers do not differ significantly (Table 6), the absorption spectra and the calculated transition energies of the studied substances cannot show which of the tautomeric forms predominates in solution.

The computations, performed for the purpose of assignment of the main chromophore, lead to the same qualitative conclusions for the compounds investigated. That is why only the quantitative results for **6** will be presented.

Drawing on the principle of structural analogy, several fragments may be studied as candidates for the main chromophore in each of the studied molecules. Figure 2 shows the fragments considered as main chromophores of 3-(2-benzthiazolyl)-coumarin **6**.

It will be shown below that model I is physically inadequate experimentally and theoretically. The spectrum of **6** cannot be regarded as a superposition of the spectra of coumarin and benzthiazole. The longest-wavelength transition of **B** is at 3.83 eV and

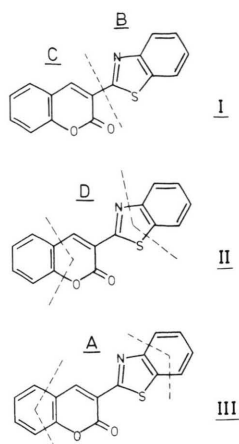


Fig. 2. Sub-systems (sub-chromophores) in the 3-(2-benzthiazolyl)-coumarin molecule, considered as main chromophores. The dashed lines denote the interrupted bonds for which the resonance integrals β in the MIM method are zero.

Table 7. Results from the application of the Pars-orbital analysis to the coumarin (**C**) and the benzthiazolyl (**B**) fragments of the molecule **6**. dL (**C**) and dL (**B**) denote the coefficients which characterize the degree of localization of the transition in the fragments **C** and **B** respectively, dCT denotes the coefficient which characterizes the degree of the CT-transition.

Transition ${}^1S_0 - {}^1S_1$	dL (C)	dL (B)	dCT
1	0.630	0.246	0.074
2	0.002	0.439	0.533
3	0.689	0.159	0.121
4	0.167	0.159	0.216

is of very low intensity [20], the energy of the longest-wavelength transition of **C** is also too high: 3.96 eV [20]. Both the experimental and the computed energies of the longest-wavelength $\pi\pi^*$ transitions of coumarin and benzthiazole differ significantly from those of **6**. This means that the transitions are localized neither in **C** nor in **B** (see also Table 7).

The application of the MIM (molecule in molecule) method of Longuet-Higgins-Murrell (see [21, 22]), where the basic π -molecular orbitals are those of the coumarin and the benzthiazolyl, shows that the configurations corresponding to intrafragmental and interfragmental CT transitions are strongly mixed. Consequently, according to the MIM

method too, neither the coumarin **C** nor the benzthiazolyl **B** fragments can be regarded as separate subchromophores.

The validity of the above conclusions can be checked by means of the pars-orbital analysis (POA) [23, 24], which gives information about the degree of localization of the transitions in different fragments of the molecule, as well as the degree of charge-transfer (CT transitions) between the fragments. Table 7 shows the results for the first six singlet transitions of **6**, obtained using basis functions from the SCF-PPP calculations. It can be seen that neither of the transition is a localized nor a CT one: all coefficients $d < 0.7$ while for the typical localized and CT transitions $d > 0.85$ [25].

The considered fragmentation of the molecule (model I) is related also to the existence of CT transitions. The performed POA (Table 7), as well as the insubstantial change of the total π -electron charges of the fragments **C** and **B** indicate that the excitation of **6** to the first three singlet $\pi\pi^*$ states does not lead to a charge transfer between **C** and **B**.

The total π -electron charge Q of the coumarin fragment in the ground state $Q({}^1S_0)$ and in the fluorescent state $Q({}^1S_1)$ is

$$Q({}^1S_0) = \sum_{i=1}^{11} q_i^{\pi}({}^1S_0) = 11.987,$$

$$Q({}^1S_1) = \sum_{i=1}^{11} q_i^{\pi}({}^1S_1) = 12.061.$$

The value and the direction of the dipole moment does not change much either: $\mu({}^1S_0) = 4.04D$, $\mu({}^1S_1) = 3.57D$. The angle between the two moments is 6° . These results refer to **6a** (see Table 6). The dipole moment of **6b** in the ground state is $\mu({}^1S_0) = 5.44D$.

In the first excited $\pi\pi^*$ singlet state only the order (P) of the bond between the fragments **C** and **B** changes substantially relative to that in the ground state: $P({}^1S_0) = 0.343$, $P({}^1S_1) = 0.516$.

The results for model II, fragment **D**, obtained by means of the MIM method, as well as the PPP-calculations are in neither quantitative nor qualitative agreement with the transition energies. E.g. the PPP method gives the following values of the longest-wavelength $\pi\pi^*$ transition energies and oscillator strengths (in parenthesis): $E_1 = 3.72$ eV (0.053), $E_2 = 5.05$ eV (0.376), $E_3 = 5.17$ eV (0.252). The comparison of the above results with the ones

given in Table 6 shows that fragment **D** cannot be regarded as a main chromophore.

The smallest structural unit in Fig. 2 which reproduces satisfactory the spectrum of **6** is 3-(2-thiazolyl)-2H-pyran-2-one fragment **A**: model III. This can be seen from Table 8, where the computed longest-wavelength $\pi\pi^*$ transition energies and oscillator strengths of **6** and fragment **A** are compared.

It should be noted, that the coincidence of the computed transition energies for a system and its subsystem (chromophore) may be incidental (22). But this is not so in the case considered by us.

The first argument supporting this conclusion is the identical character of the transitions of **6** and **A**. Let us denote the expansion of the wave function into configurations by

$$\Phi = \sum_{i, k'} c_{ik'} V_{ik'}, \quad (1)$$

where $V_{ik'}$ is the configuration obtained upon electron transition from the i -th occupied MO the k' -th vacant MO. $V_{11'}$ is the configuration with an electron transfer from the HOMO (ψ_1) to the LUMO ($\psi_{1'}$). Configuration analysis (Table 8) shows that both the energies and the character of the first transitions of **6** and **A** are identical.

Another argument in favor of the assignment of **A** as the main chromophore is the coincidence of the longest-wavelength transition polarization of **6** and **A**: Figure 3.

Table 8. Computed energies ΔE [eV] of the longest-wavelength $^1S_0 - ^1S_1$ ($\pi\pi^*$) transitions, oscillator strengths f and coefficients of the configurations of greatest statistical weight for **6** and fragment **A**.

ΔE	f	Coefficients of the dominating configurations
6		
3.25	1.079	$0.95 V_{11'} + 0.11 V_{21'} + 0.20 V_{31'}$
^a 3.82	0.062	$0.10 V_{11'} - 0.90 V_{21'} + 0.14 V_{31'}$
A		
3.26	0.688	$0.97 V_{11'} + 0.18 V_{21'}$
^b 4.16	0.039	$0.17 V_{11'} - 0.95 V_{21'}$

^a $\Delta E (^3T_1) = 1.21$ [eV]. ^b $\Delta E (^3T_1) = 1.01$ [eV].

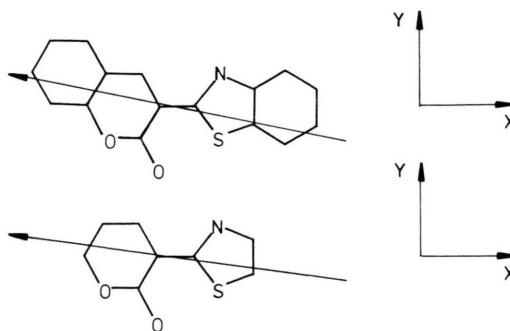


Fig. 3. Direction of the computed transition moment Q of the longest-wavelength $^1S_0 - ^1S_1$ ($\pi\pi^*$) transition of **6** and the fragment **A**.

- [1] M. Maeda, *Laser Dyes*, Academic Press, New York 1984.
- [2] R. Raue, H. Jarnisch, and K. Drexhage, *Heterocycles* **21** (No. 1) 167 (1984).
- [3] O. Wolfbeis, W. Rapp, and E. Lippert, *Monatsh. Chem.* **109**, 899 (1978).
- [4] B. Krasovitskii and B. Bolotin, *Organic Luminescences* (Russ.), Khimia, Leningrad, Ed. 1976, USSR.
- [5] O. Wolfbeis, E. Furlinger, H. Kooneis, and H. Marschner, *Fresenius Z. Anal. Chemie* **314**, 119 (1983).
- [6] H. Hagen and R. Kohler, *Ger. Offen.* **2**, 950, 291 (1981), BASF A.G.
- [7] V. Dryanska, *Synth. Commun.* **17**, 203 (1987).
- [8] N. Borisovitch, V. Zelinskii, and B. Neporent, *Dokl. Acad. Nauk USSR* **94**, 37 (1954).
- [9] T. Azumi and S. P. McGlynn, *J. Chem. Phys.* **37**, 2413 (1962).
- [10] F. Perrin, *J. Phys. Radium* **7**, 390 (1926).
- [11] T. Moore, M. Harter, and P. Song, *J. Mol. Spectroscopy* **40**, 144 (1971).
- [12] P. Petrovitch and N. Borisevitch, *Izv. Acad. Nauk USSR, Ser. Phys.* **27**, No. 5, 703 (1963).
- [13] M. El-Sayed and G. Robinson, *J. Chem. Phys.* **34**, 1840 (1961).
- [14] Patent Bulg. reg. No. 71328, 01.08.1985.
- [15] E. Lipert, *Z. Elektrochem.* **61**, 962 (1957).
- [16] V. Balaiah, T. Seshadri, and V. Venkateswalu, *Proc. Indian Acad. Sci.* **16A**, 68 (1942).
- [17] N. Tyutyulkov and G. Hiebaum, *Theor. Chim. Acta Berlin* **14**, 39 (1969).
- [18] J. Fabian, K. Fabian, and H. Hartmann, *Theor. Chim. Acta Berlin* **12**, 319 (1968).
- [19] C. A. Coulson and A. Golebiewski, *Proc. Phys. Soc. London* **78**, 1310 (1961).
- [20] L. Lang (Ed.), *Absorption Spectra in the UV-VIS Region*, Publishing House of the Hungarian Acad. Sci. Budapest 1961, **II**, p. 371 and p. 367.
- [21] J. Fabian, *J. Signalaufzeichnungsmaterialien* **6**, 307 (1978); **7**, 67 (1979).
- [22] J. Fabian, A. Mehlhorn, F. Dietz, and N. Tyutyulkov, *M. H. Chemie* **115**, 21 (1984).
- [23] O. E. Polansky and G. Derflinger, *Int. J. Quantum Chem.* **1**, 379 (1967).
- [24] O. E. Polansky, *Z. Naturforsch.* **29a**, 529 (1974).
- [25] F. Fratev, V. Enchev, P. Nikolov, and O. E. Polansky, *Z. Naturforsch.* **39a**, 1143 (1984).